THREE-DIMENSIONAL NUMERICAL MODEL FOR FULLY NONLINEAR WAVES OVER ARBITRARY BOTTOM

Philippe Guyenne [1], Stéphan T. Grilli [2], M.ASCE, and Frédéric Dias [3]

Abstract: We present an accurate three-dimensional (3D) Numerical Wave Tank (NWT) solving the full equations in the potential flow formulation. The NWT is able to simulate wave propagation up to overturning over an arbitrary bottom topography. The model is based on a high-order 3D Boundary Element Method (BEM) with the Mixed Eulerian-Lagrangian (MEL) approach. The spatial discretization is third-order and ensures continuity of the inter-element slopes. Waves can be generated in the tank by wavemakers or they can be directly specified on the free surface. A node regridding can be applied at any time step over selected areas of the free surface. Results are presented for the computation of overturning waves over a ridge and their kinematics.

INTRODUCTION

Many numerical wave models solving Fully Nonlinear Potential Flow (FNPF) equations have been developed, mostly in two dimensions (2D), which have been shown to accurately simulate wave overturning in deep and intermediate water (Dommermuth et al. 1988) as well as wave shoaling and breaking over slopes (Grilli et al. 1997). In most recent 2D models, incident waves can be generated at one extremity and reflected, absorbed or radiated at the other extremity (Grilli and Horrillo 1997). In three dimensions (3D), only a few attempts have been reported of solving FNPF problems, for arbitrary transient nonlinear waves in a general propagation model, with the possibility of modeling overturning waves. Xu and Yue (1992) and Xue et al. (2001) calculated 3D overturning waves in a doubly periodic computational domain with infinite depth (i.e. only the free surface was discretized). In their case, progressive Stokes waves were led to breaking

[1]Dept. of Math. and Stat., McMaster Univ., Hamilton, ON L8S 4K1, Canada. E-mail: guyenne@math.mcmaster.ca.
[2]Ocean Engrg. Dept., Univ. of Rhode Island, Narragansett, RI 02882, USA. E-mail: grilli@oce.uri.edu.
[3]CMLA, ENS de Cachan, 94235 Cachan cedex, France. E-mail: dias@cmla.ens-cachan.fr.

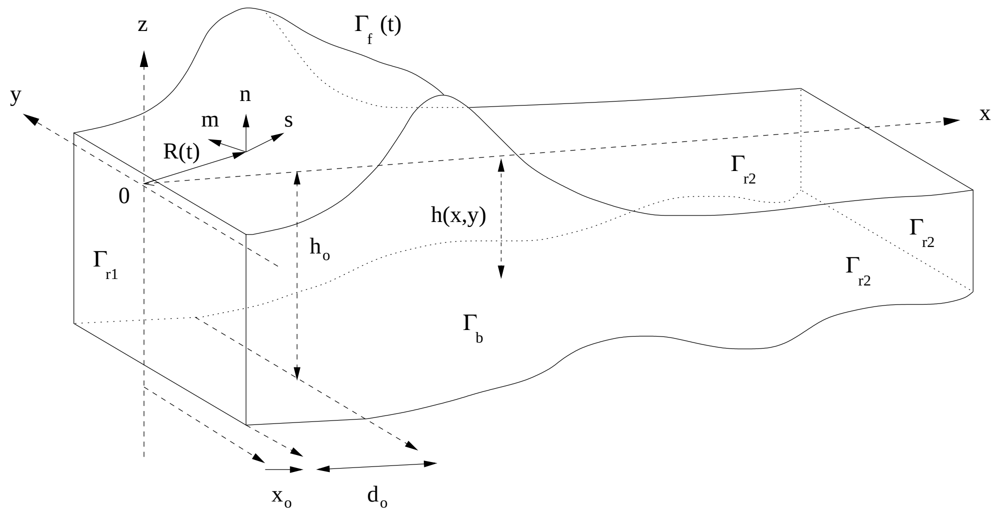

FIG. 1. Sketch of the computational domain for the 3D BEM.

by specifying an asymmetric surface pressure. Sawtooth instabilities eventually developed near the wave crests and were eliminated by smoothing. Broeze (1993) developed a numerical model similarly to Xu and Yue's but for non-periodic domains and finite depth. He was able to produce the initial stages of wave overturning over a bottom shoal. Numerical instabilities were also experienced which limited the computations.

In the present study, we propose a new 3D nonlinear surface wave model (Fig. 1), solving FNPF equations based on a high-order 3D Boundary Element Method (BEM) and a mixed Eulerian-Lagrangian time updating of the free surface Γ_f. The methods used for both spatial and temporal discretizations are direct 3D extensions of those in Grilli and Subramanya (1996). The model is applicable to nonlinear wave transformations up to overturning and breaking from deep to shallow water of arbitrary bottom topography Γ_b. This, in fact, constitutes a Numerical Wave Tank (NWT), where arbitrary waves can be generated by wavemakers on Γ_{r1} or they can be directly specified on the free surface. If needed, absorbing boundary conditions can be simulated on lateral boundaries Γ_{r2} (Grilli and Horrillo 1997). In addition, techniques are developed for regridding nodes at any time step, over selected areas of the free surface.

MATHEMATICAL FORMULATION

Equations for the FNPF formulation with a free surface are summarized below. The fluid velocity is expressed as $\boldsymbol{u} = \boldsymbol{\nabla}\phi = (u, v, w)$, with $\phi(\boldsymbol{x}, t)$ the velocity potential.

Continuity equation in the fluid domain $\Omega(t)$, with boundary $\Gamma(t)$, is Laplace's equation for the velocity potential,

$$\nabla^2\phi = 0\,. \qquad (1)$$

The 3D free space Green's function for Eq. (1) is defined as

$$G(\boldsymbol{x}, \boldsymbol{x}_l) = \frac{1}{4\pi r} \quad \text{and} \quad \frac{\partial G}{\partial n}(\boldsymbol{x}, \boldsymbol{x}_l) = -\frac{1}{4\pi} \frac{\boldsymbol{r} \cdot \boldsymbol{n}}{r^3}, \tag{2}$$

with $r = |\boldsymbol{r}| = |\boldsymbol{x} - \boldsymbol{x}_l|$ the distance from the source point $\boldsymbol{x}$ to the field point $\boldsymbol{x}_l$ (both on boundary Γ) and $\boldsymbol{n}$ the outward unit normal vector at $\boldsymbol{x}$ on Γ.

Green's second identity transforms Eq. (1) into the Boundary Integral Equation (BIE)

$$\alpha(\boldsymbol{x}_l)\, \phi(\boldsymbol{x}_l) = \int_\Gamma \left\{ \frac{\partial \phi}{\partial n}(\boldsymbol{x})\, G - \phi(\boldsymbol{x})\, \frac{\partial G}{\partial n} \right\} \mathrm{d}\Gamma, \tag{3}$$

where $\alpha(\boldsymbol{x}_l) = \theta_l/(4\pi)$ with θ_l the exterior solid angle at point $\boldsymbol{x}_l$.

The boundary is divided into various sections, with different boundary conditions (Fig. 1). On the free surface $\Gamma_f(t)$, ϕ satisfies the nonlinear kinematic and dynamic boundary conditions

$$\frac{D\,\boldsymbol{R}}{D\,t} = \boldsymbol{u} = \boldsymbol{\nabla}\phi, \tag{4}$$

$$\frac{D\,\phi}{D\,t} = -gz + \frac{1}{2}\,\boldsymbol{\nabla}\phi \cdot \boldsymbol{\nabla}\phi - \frac{p_a}{\rho}, \tag{5}$$

respectively, with $\boldsymbol{R}$ the position vector of a fluid particle on the free surface, g the acceleration due to gravity, p_a the atmospheric pressure, ρ the fluid density and D/Dt the Lagrangian time derivative.

Various methods can be used in the NWT for wave generation. When waves are generated by a wavemaker at the "open sea" boundary $\Gamma_{r1}(t)$, motion and velocity $[\boldsymbol{x}_p(t), \boldsymbol{u}_p(t)]$ are specified over the wavemaker as

$$\overline{\boldsymbol{x}} = \boldsymbol{x}_p \qquad \text{and} \qquad \overline{\frac{\partial \phi}{\partial n}} = \boldsymbol{u}_p \cdot \boldsymbol{n}, \tag{6}$$

where overlines denote specified values.

Along the bottom Γ_b and other fixed parts of the boundary referred to as Γ_{r2}, a no-flow condition is prescribed as

$$\overline{\frac{\partial \phi}{\partial n}} = 0. \tag{7}$$

The solution within the domain can be easily evaluated from the boundary values. For instance, the internal velocity and local acceleration are given by

$$\boldsymbol{\nabla}\phi(\boldsymbol{x}_l) = \int_\Gamma \left\{ \frac{\partial \phi}{\partial n}(\boldsymbol{x})\, Q - \phi(\boldsymbol{x})\, \frac{\partial Q}{\partial n} \right\} \mathrm{d}\Gamma, \tag{8}$$

$$\boldsymbol{\nabla}\frac{\partial \phi}{\partial t}(\boldsymbol{x}_l) = \int_\Gamma \left\{ \frac{\partial^2 \phi}{\partial t \partial n}(\boldsymbol{x})\, Q - \frac{\partial \phi}{\partial t}(\boldsymbol{x})\, \frac{\partial Q}{\partial n} \right\} \mathrm{d}\Gamma,$$

respectively, where

$$Q(\boldsymbol{x},\boldsymbol{x}_l) = \frac{1}{4\pi\, r^3}\,\boldsymbol{r} \qquad \text{and} \qquad \frac{\partial Q}{\partial n}(\boldsymbol{x},\boldsymbol{x}_l) = \frac{1}{4\pi\, r^3}\left\{\boldsymbol{n} - 3\,(\boldsymbol{e}_r\cdot\boldsymbol{n})\,\boldsymbol{e}_r\right\},$$

with $\boldsymbol{e}_r = \boldsymbol{r}/r$.

Note, results presented here only have no-flow conditions on lateral boundaries Γ_{r1} and Γ_{r2}. For the use of a "snake" flap wavemaker and an absorbing piston at extremities of the tank, the reader can refer to Brandini and Grilli (2001).

TIME INTEGRATION

Following the method implemented in Grilli and Subramanya's 2D model (1996), second-order explicit Taylor series expansions are used to express both the new position $\overline{\boldsymbol{R}}(t+\Delta t)$ and the potential $\overline{\phi}(\boldsymbol{R}(t+\Delta t))$ on the free surface, in the MEL formulation, as

$$\overline{\boldsymbol{R}}(t+\Delta t) = \boldsymbol{R} + \Delta t \frac{D\,\boldsymbol{R}}{D\,t} + \frac{(\Delta t)^2}{2}\frac{D^2\boldsymbol{R}}{Dt^2} + \mathcal{O}[(\Delta t)^3]\,, \tag{9}$$

$$\overline{\phi}(\boldsymbol{R}(t+\Delta t)) = \phi + \Delta t \frac{D\,\phi}{D\,t} + \frac{(\Delta t)^2}{2}\frac{D^2\phi}{Dt^2} + \mathcal{O}[(\Delta t)^3]\,, \tag{10}$$

where all terms in the right-hand sides are calculated at time t.

Coefficients in these Taylor series are expressed as functions of the potential, its partial time derivative, as well as the normal and tangential derivatives of both of these along the free surface. Thus, the first-order coefficients are given by Eqs. (4) and (5), which requires calculating $(\phi, \frac{\partial\phi}{\partial n})$ on the free surface. The second-order coefficients are obtained from the Lagrangian time derivative of Eqs. (4) and (5), which requires also calculating $(\frac{\partial\phi}{\partial t}, \frac{\partial^2\phi}{\partial t\partial n})$ at time t.

As in Grilli and Svendsen (1990), the time step Δt in Eqs. (9) and (10) is adapted at each time as a function of the minimum distance between two nodes on the free surface and a constant mesh Courant number $\mathcal{C}_o \simeq 0.45$.

The advantages of this time stepping scheme are of being explicit and using spatial derivatives of the field variables along the free surface in the calculation of values at $(t+\Delta t)$. This provides for a better stability of the computed solution and makes it possible to use larger time steps, for a similar accuracy, than in Runge-Kutta or predictor-corrector methods, which only use point to point updating based on time derivatives and thus are more subject to sawtooth instabilities. Hence, this also makes the overall solution more efficient for a specified numerical accuracy of the results.

BOUNDARY DISCRETIZATION AND REGRIDDING

The BIEs for ϕ and $\frac{\partial\phi}{\partial t}$ are solved by a BEM. The boundary is discretized into collocation nodes and M_Γ high-order elements are used to interpolate in between m of these nodes. Within each element, the boundary geometry and the field variables (denoted by $u = \phi$ or $\frac{\partial \phi}{\partial t}$, and $q = \frac{\partial \phi}{\partial n}$ or $\frac{\partial^2 \phi}{\partial t \partial n}$, for simplicity) are discretized using polynomial shape functions $N_j(\xi, \eta)$ as

$$\boldsymbol{x}(\xi, \eta) = N_j(\xi, \eta)\, \boldsymbol{x}_j^k$$

$$u(\xi, \eta) = N_j(\xi, \eta)\, u_j^k \quad , \quad q(\xi, \eta) = N_j(\xi, \eta)\, q_j^k$$

where $j = 1, \ldots, m$ denotes the nodes within each element $k = 1, \ldots, M_\Gamma$. The summation convention is applied to repeated subscripts.

Isoparametric elements can provide a high-order approximation within their area of definition but only offer C_0 continuity of the geometry and field variables at nodes in between elements. Based on the experience in modeling overturning waves in 2D NWTs, for producing stable accurate results one needs to define elements which are both higher-order within their area of definition and at least locally C_2 continuous in between elements. Here, the elements are defined using an extension of the so-called Middle-Interval-Interpolation (MII) method introduced by Grilli and Subramanya (1996). The boundary elements are 4-node quadrilaterals with cubic shape functions defined using both these and additional neighboring nodes in each direction for a total of $m = 16$ nodes.

The discretized boundary integrals are calculated for each collocation node by numerical integration. When the collocation node does not belong to the integrated element, a standard Gauss-Legendre quadrature method is used. When it belongs to the element, the distance r in the Green's function and in its normal gradient becomes zero at one of the nodes of the element (Eq. (2)). It can be shown that the integrals including G are weakly singular whereas the integrals including $\frac{\partial G}{\partial n}$ are non-singular. For the former integrals, a method of "singularity extraction", well-suited to MII elements, is applied based on polar coordinate and other transformations.

The linear algebraic system resulting from the discretization of Eq. (3) for ϕ (and $\frac{\partial \phi}{\partial t}$) is in general dense and non-symmetric. Since the number of nodes N_Γ can be very large in 3D, the solution by a direct method of order $\mathcal{O}(N_\Gamma^3)$ is prohibitive. As in Xu and Yue (1992) and Xue et al. (2001), a preconditioned GMRES (Generalized Minimal Residual) algorithm is used to iteratively solve the linear system.

Two types of regridding methods for the free surface are included in the model. When the free surface is still single-valued, a 2D horizontal regridding to a finer resolution can be performed in selected areas of the free surface. It consists in a reinterpolation of nodes for equally spaced MII elements in the x and y directions. In addition, we developed a local regridding technique similar to that in Grilli and Subramanya (1996) which redistributes the nodes in regions of flow convergence like in the breaker jet. When the distance between 2 nodes on grid lines along the direction of wave propagation becomes too small in comparison with the distance between neighboring nodes, the nodes are locally regridded to make these distances equal. The purpose is to limit the occurrence of quasi-singular integrals in the BIEs, resulting from the node convergence. Note, for regridding, the same

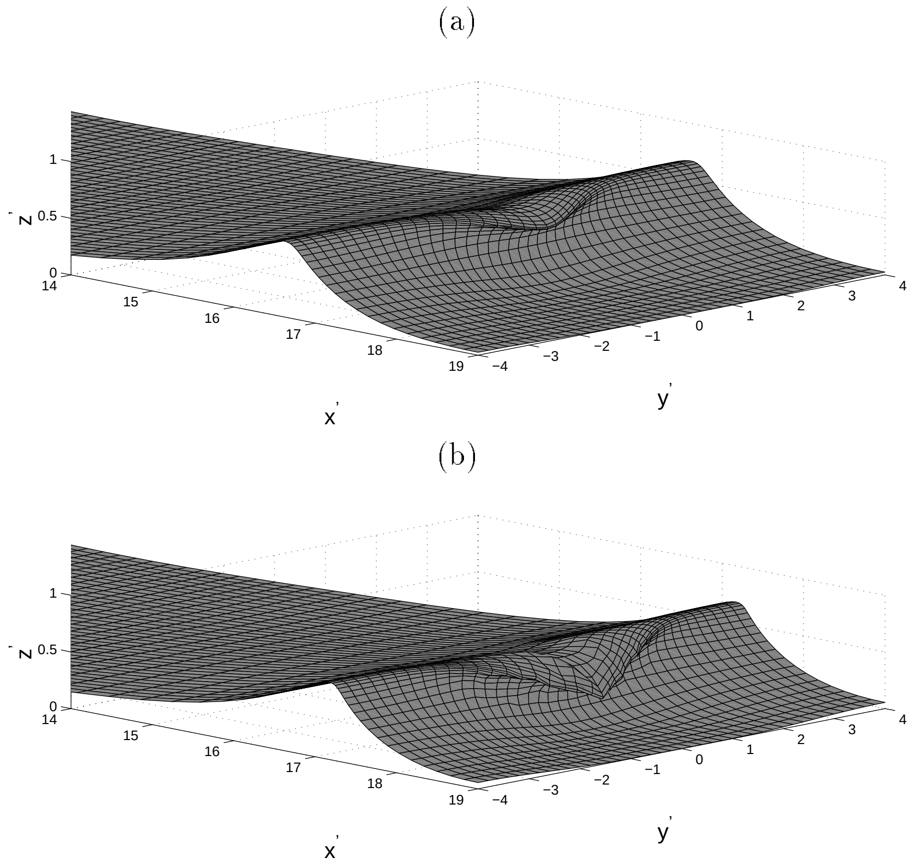

FIG. 2. Wave profiles over a sloping ridge, at t' = (a) 8.577 and (b) 8.997.

interpolation functions as in the BEM are used to recalculate the solution at the new nodes, without modifying the solution obtained at the old nodes.

The reader can refer to Grilli et al. (2001) for more details on the model (description, validation, etc.).

RESULTS: SOLITARY WAVE SHOALING AND BREAKING OVER A SLOPING RIDGE

A domain of depth h_o and width $8h_o$ in the y direction is considered, with a sloping ridge at its x extremity. The ridge starts at $x' = 5.225$ and has a 1:15 slope in the middle ($y' = 0$), tapered in the y direction by specifying a depth variation in the form of a sech^2 modulation. The ridge is truncated at $x' = 19$ where the minimum depth is $h' = 0.082$ in the middle part ($y' = 0$) and the maximum depth $h' = 0.614$ on the sides ($y' = \pm 4$). [Dashes indicate non-dimensional variables based on the long wave theory, i.e. lengths are divided by h_o and times by $\sqrt{h_o/g}$.] The initial condition is an exact FNPF solitary wave of height $H'_o = 0.6$, with its crest located at $x' = 5.7$ for $t' = 0$. Such a wave is obtained using the numerical method proposed by Tanaka (1986).

The initial BEM discretizations on the bottom and the free surface have 50 by 20 quadrilateral elements in the x and y directions, respectively ($\Delta x'_o = 0.38$

(a)

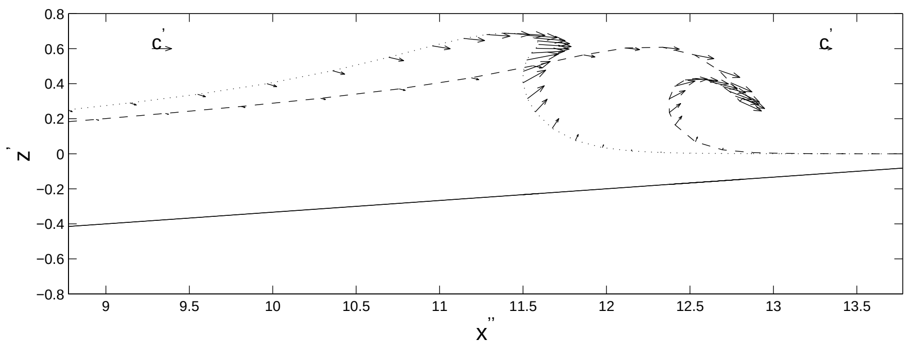

(b)

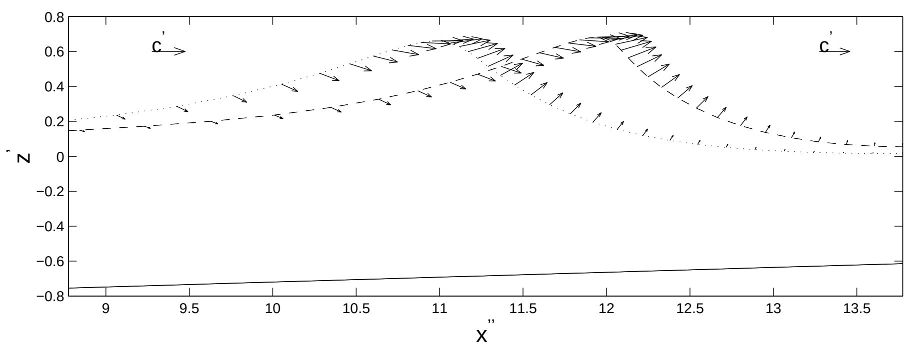

FIG. 3. Vertical cross-sections at (a) $y' = 0$ and (b) $y' = \pm\, 4$. Surface velocity field at $t' = 8.259$ (. . . .) and $t' = 8.997$ (– –).

and $\Delta y'_o = 0.40$). The total number of nodes and of quadrilateral MII elements are $N_\Gamma = 2862$ and $M_\Gamma = 2560$, respectively. The initial time step is set to $\Delta t'_o = 0.171$ ($\mathcal{C}_o = 0.45$). Maximum numerical errors of 1 % on wave mass and energy conservation are considered acceptable in this application. Computations are first performed in the initial discretization up to reaching these maximum errors. The 2D regridding of part of the NWT to a finer discretization is then specified at an earlier time $t' = 5.769$ for which errors are very small (0.012 % and 0.032 % for wave mass and energy respectively). At this stage, the wave crest is located at $x' = 13.2$ with $H' = 0.64$. The regridded discretization is increased to 60 by 40 quadrilateral elements on the free surface and bottom boundaries for $x' = 8.075$ to 19 ($\Delta x'_o = 0.182$, $\Delta y'_o = 0.20$, $N_\Gamma = 6022$, $M_\Gamma = 5600$) and computations are pursued, up to $t' = 8.577$.

Fig. 2(a) shows the wave computed at this time. Errors on wave mass and energy are still small (0.026 % and 0.054 % respectively) but the time step has considerably reduced, to $\Delta t' = 0.0016$. Wave overturning has already started in the middle of the NWT and has not yet reached the sidewalls. However, computations cannot be pursued much beyond this stage due to the node convergence at the wave crest. This problem is overcome by using the local adaptive regrid-

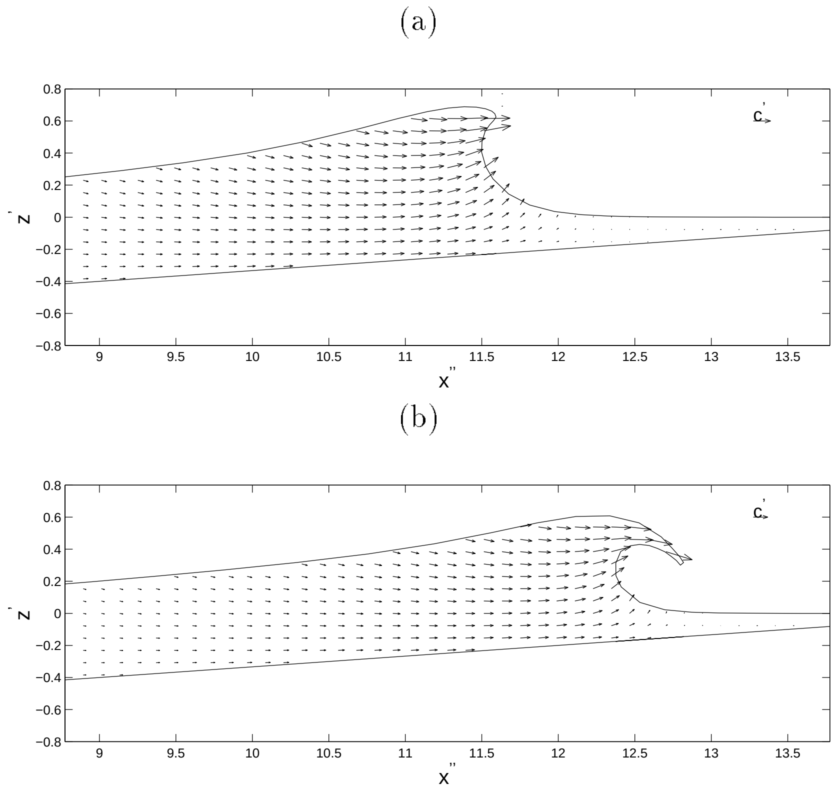

FIG. 4. Vertical cross-sections at $y' = 0$. Internal velocity field at $t' =$ (a) 8.259 and 8.997.

ding technique for nodes in the breaker jet. As a result, the solution in Fig. 2(b) exhibits a well developed plunging jet at $t' = 8.997$. One clearly sees that the overturning process tends to propagate laterally to the sidewalls. Grilli et al. (2001) evaluated the lateral mean speed of propagation of wave overturning.

Fig. 3 depicts the velocity field (u', w') in vertical sections in the middle of the NWT ($y' = 0$) and at the sidewalls ($y' = \pm 4$) for fluid particles on the free surface. The results are qualitatively in good agreement with those obtained by New et al. (1985) for overturning waves in 2D. In Fig. 4, we show the internal velocity field (u', w') for ($y' = 0$) at $t' = 8.259$ and $t' = 8.997$. This was computed by using Eq. (8). For comparison, the celerity of a linear wave in shallow water $c' = \sqrt{g' h'_o}$ is given on the figures. Finally, the horizontal internal velocity field (u', v') is shown in Fig. 5, at depth $h' = -0.2$ for $t' = 7.911$ and $t' = 8.997$. Curves represent the bottom cross-sections. Focusing of the flow by the ridge can be seen on the figures, illustrating 3D breaking effects.

CONCLUSIONS

A 3D computation of wave shoaling and overturning over an arbitrary bottom topography was presented. Our results show a better stability and numerical accuracy than in previous attempts reported in the literature for calculating such strongly nonlinear 3D surface waves. Regridding techniques are developed to

(a)

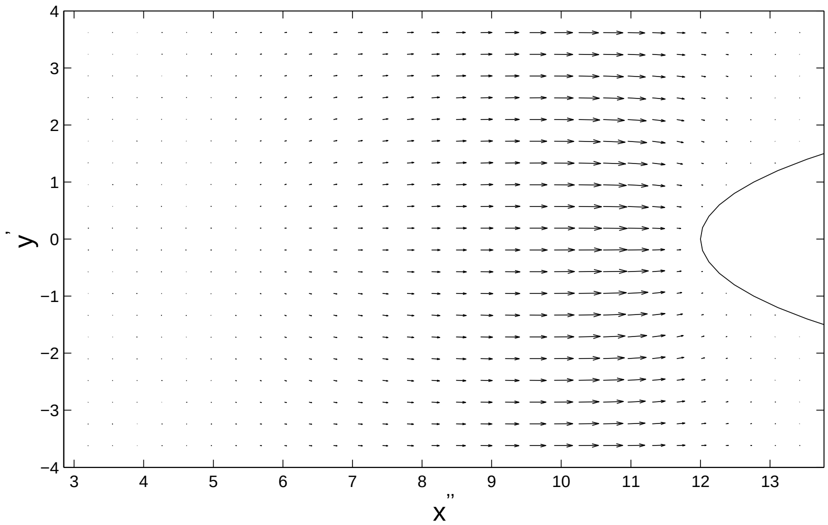

(b)

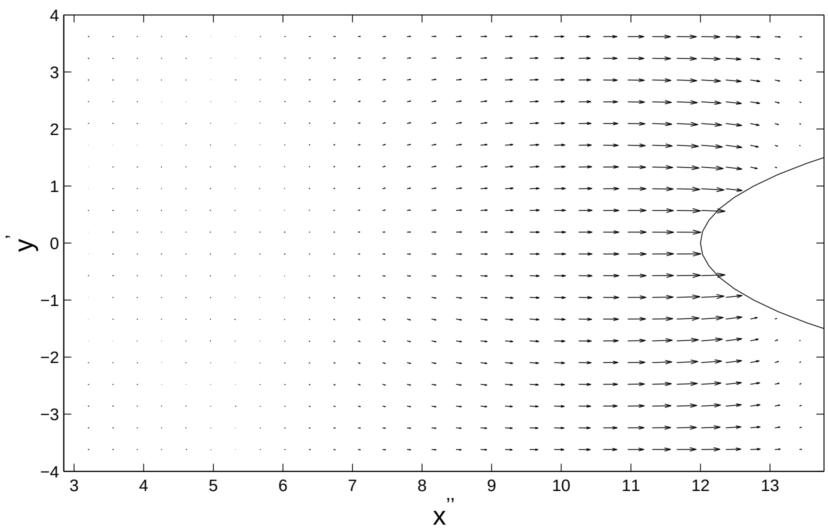

FIG. 5. Horizontal cross-sections at h' = -0.2. Internal velocity field at (a) the breaking point t' = 7.911 and (b) t' = 8.997.

describe the solution far beyond the breaking point. To our knowledge, this was never attempted before in a general 3D-NWT. The model can be applied to a wide range of problems such as the modeling of freak waves (Brandini and Grilli 2001) and the modeling of wave impact against structures (Guyenne et al. 2000).

ACKNOWLEDGMENTS

The first and third authors acknowledge support from the Délégation Générale pour l'Armement (France). The second author acknowledges support from the US Office of Naval Research, under grant N-00014-99-10439 of the Coastal Dynamics

Division (code 321 CD). Computations carried out in this research project were performed in part on the NEC SX5 supercomputer located at IDRIS, under CNRS funding.

REFERENCES

Brandini, C. and Grilli, S. T. (2001). "Modeling of freak wave generation in a 3D NWT." *Proc. 11th Offshore and Polar Engrg. Conf.*, Stavanger, Norway. 124–131.

Broeze, J. (1993). "Numerical modelling of nonlinear free surface waves with a 3D panel method," Phd dissertation, Enschede, The Netherlands.

Dommermuth, D. G., Yue, D. K. P., Lin, W. M., Rapp, R. J., Chan, E. S., and Melville, W. K. (1988). "Deep-water plunging breakers: a comparison between potential theory and experiments." *J. Fluid Mech.*, 189, 423–442.

Grilli, S. T., Guyenne, P., and Dias, F. (2001). "A fully nonlinear model for three-dimensional overturning waves over arbitrary bottom." *Int. J. Numer. Meth. Fluids*, 35, 829–867.

Grilli, S. T. and Horrillo, J. (1997). "Numerical generation and absorption of fully nonlinear periodic waves." *J. Engrg. Mech.*, 123(10), 1060–1069.

Grilli, S. T. and Subramanya, R. (1996). "Numerical modeling of wave breaking induced by fixed or moving boundaries." *Computational Mech.*, 17, 374–391.

Grilli, S. T. and Svendsen, I. A. (1990). "Corner problems and global accuracy in the boundary element solution of nonlinear wave flows." *Engrg. Analysis with Boundary Elements*, 7(4), 178–195.

Grilli, S. T., Svendsen, I. A., and R., S. (1997). "Breaking criterion and characteristics for solitary waves on slopes." *J. Waterways Port Coastal and Ocean Engrg.*, 123(3), 102–112.

Guyenne, P., Grilli, S. T., and Dias, F. (2000). "Numerical modeling of fully nonlinear 3D overturning waves over arbitrary bottom." *Proc. 27th Int. Conf. on Coastal Engrg.*, Sydney, Australia. 1–12.

New, A. L., McIver, P., and Peregrine, D. H. (1985). "Computation of overturning waves." *J. Fluid Mech.*, 150, 233–251.

Tanaka, M. (1986). "The stability of solitary waves." *Phys. Fluids*, 29(3), 650–655.

Xu, H. and Yue, D. K. P. (1992). "Computations of fully nonlinear three-dimensional water waves." *Proc. 19th Symp. on Naval Hydrodynamics*, Seoul, Korea. 1–24.

Xue, M., Xu, H., Liu, Y., and Yue, D. K. P. (2001). "Computations of fully nonlinear three-dimensional wave-wave and wave-body interactions. Part 1. Dynamics of steep three-dimensional waves." *J. Fluid Mech.*, 438, 11–39.